JACC Vol. 27, No. 7
June 1996:1577–85

Myocyte Degeneration and Cell Death in Hibernating Human Myocardium

ERNST R. SCHWARZ, MD, JUTTA SCHAPER, MD,* JUERGEN VOM DAHL, MD, CARSTEN ALTEHOEFER, MD, BEATE GROHMANN, TA,* FRIEDRICH SCHOENDUBE, MD, MS, FLORENCE H. SHEEHAN, MD,† RAINER UEBIS, MD, UDALRICH BUELL, MD, BRUNO J. MESSMER, MD, FACC, WOLFGANG SCHAPER, MD,* PETER HANRATH, MD, FACC

Aachen and Bad Nauheim, Germany; and Seattle, Washington

Objectives. **The aim of this study was to analyze the morphologic characteristics of myocyte degeneration leading to replacement fibrosis in hibernating myocardium by use of electron microscopy and immunohistochemical techniques.**

Background. **Data on the ultrastructure and the cytoskeleton of cardiomyocytes in myocardial hibernation are scarce. Incomplete or delayed functional recovery might be due to a variable degree of cardiomyocyte degeneration in hibernating myocardium.**

Methods. **In 24 patients, regional wall motion abnormalities were analyzed by use of the centerline method before and 6 ± 1 months after coronary artery bypass surgery. Preoperative technetium-99m sestamibi uptake was measured by single-photon emission computed tomography for assessing regional perfusion. Fluorine-18 fluorodeoxyglucose uptake was measured by positron emission tomography to assess glucose metabolism. Transmural biopsy specimens were taken during coronary artery bypass surgery from the center of the hypocontractile area of the anterior wall.**

Results. **The myocytes showed varying signs of mild-to-severe degenerative changes and an increased degree of fibrosis. Immunohistochemical analysis demonstrated disruption of the cytoskeletal proteins titin and alpha-actinin. Electron microscopy of the cell organelles and immunohistochemical analysis of the cytoskeleton showed a similarity in the degree of degenerative alterations. Group 1 (n = 11) represented patients with only minor structural alterations, whereas group 2 (n = 13) showed severe morphologic degenerative changes. Wall motion abnormalities showed postoperative improvements, and nuclear imaging revealed a perfusion-metabolism mismatch without significant differences between the groups.**

Conclusions. **Long-term hypoperfusion causes different degrees of morphologic alterations leading to degeneration. Preoperative analysis of regional contractility and perfusion-metabolism imaging does not distinguish the severity of morphologic alterations nor the functional outcome after revascularization. The insufficient act of self-preservation in hibernating myocardium may lead to a progressive structural degeneration with an incomplete and delayed recovery of function after restoration of blood flow.**

(J Am Coll Cardiol 1996;27:1577–85)

Long-term reduction of coronary blood flow is associated with reduced contraction and altered cellular metabolism but with improved or normalized regional dysfunction after successful revascularization, termed *myocardial hibernation* (1–3). Improvement of wall motion in hibernating myocardium can be achieved by coronary revascularization by either angioplasty (4–7) or coronary artery bypass surgery (8–11). Preoperative metabolic imaging by positron emission tomography has recently been shown to predict recovery of regional wall motion and thus maintain myocardial viability (4,9,12–14). That contractile function can resume rather quickly (15) or can be delayed after blood flow has been restored indicates a time dependence of structural remodeling to rebuild energy stores and cellular contractile material (16). Histologic studies are scarce and show moderate morphologic alterations and a slight increase of connective tissue (17–23). In the present study, morphologic characteristics of myocardial hibernation were assessed by electron microscopy and immunohistochemical techniques.

Methods

Patients. Twenty-four patients (21 men, 3 women; mean [±SD] age 60 ± 8 years, range 43 to 71) underwent coronary angiography and biplane left ventricular angiography. Patients prospectively recruited fulfilled the following inclusion criteria:

From the Medical Clinic I, Departments of Cardiology, Nuclear Medicine and Cardiovascular Surgery, Rheinisch-Westfälische Technische Hochschule University Hospital, Aachen and *Department of Experimental Cardiology, Max-Planck-Institute, Bad Nauheim, Germany; and †Cardiovascular Research and Training Center, University of Washington, Seattle, Washington.

Manuscript received September 13, 1995; revised manuscript received January 12, 1996, accepted January 30, 1996.

Address for correspondence: Dr. Ernst R. Schwarz, Medical Clinic I, Department of Cardiology, Rheinisch-Westfälische Technische Hochschule University Hospital, Pauwelsstrasse 30, 52057 Aachen, Germany.

0735-1097/96/$15.00
PII S0735-1097(96)00059-9

1) anterior wall motion abnormalities; 2) stenosis (>70%) or occlusion of the left anterior descending coronary artery; 3) angina pectoris symptoms and objective electrocardiographic (ECG) criteria for ischemia at rest or during exercise; 4) clinical indication for coronary revascularization; 5) coronary anatomy suitable for coronary artery bypass surgery; 6) persistent R waves in the anterior leads of the ECG; 7) absence of any history or ECG changes for previous anterior transmural infarction; 8) evidence for reduced perfusion but maintained viability of the anterior wall by nuclear imaging.

The study protocol had been approved by the institutional ethical review board, and patients gave written informed consent before participation.

Coronary and left ventricular angiography and regional wall motion analysis. Cardiac catheterization was performed by use of Judkins technique, and angiograms were recorded on 35-mm cine film with 50 frames/s for further quantitative analysis. Left ventricular angiography at baseline and at follow-up was obtained in the 30° right anterior oblique and 60° left anterior oblique view using 40 ml iopamidol (612 mg/ml) injected at 15 ml/s. Quantitative analysis of the ventriculograms, without knowledge of clinical or nuclear data in randomized order, was performed at the Cardiovascular Training and Research Center, University of Washington, Seattle, Washington. Left ventricular volume and global ejection fraction were calculated by the area length method (24). Regional wall motion in the distribution territory of the left anterior descending coronary artery was analyzed from the right anterior oblique projection using the centerline method and is expressed in units of standard deviation of the normal mean (25,26). Wall motion was computed as the mean motion of chords lying in the most abnormally contracting region (left anterior descending coronary artery center), whereas wall motion of the remaining left anterior descending coronary artery territory was defined as left anterior descending coronary artery periphery.

Nuclear imaging. Nuclear imaging of myocardial perfusion and metabolism followed standard protocols at our institution (27,28). Imaging was performed 2 ± 2 weeks after coronary angiography and 2 ± 2 weeks before bypass surgery.

Single-photon emission computed tomography (SPECT). Patients were studied at rest after injection of 10 mCi of technetium (Tc)-99m sestamibi (Cardiolite, DuPont). Imaging was initiated 1 to 2 h later after a light meal to reduce gastrointestinal activity. Data were acquired using a Gammasonics ROTA double-head camera (Siemens) equipped with a low-energy all-purpose collimator allowing a simultaneous 360° rotation (180° for each camera head) with 2 × 30 steps of 6° each. Transaxial slices (6.25-mm thickness) were reconstructed using a Butterworth filter third order and a cut-off frequency of 0.5 on a MaxDelta computer system (Siemens, Germany).

Positron emission tomography. A transmission scan was performed before metabolic imaging to correct for tissue photon attenuation using a retractable germanium-68 source. After oral glucose loading with 50 g of dextrose, 6 to 8 mCi of fluorodeoxyglucose (Department of Radiochemistry, Nuclear Research Center, Juelich, Germany) were injected intravenously as a slow bolus. After the tracer was injected, static ungated imaging was initiated 30 to 45 min using an ECAT 953/15 scanner (Siemens) and lasted for 30 to 40 min. Because of the one-block ring configuration of the scanner providing 15 transaxial slices over a 5-cm field of view, at least two adjacent bed positions were necessary to cover the entire heart. Transaxial images were reconstructed with a Hanning filter (cutoff frequency 0.4) in a 64 × 64 matrix and a defined zoom factor of 1.2446 to obtain the same in-plane pixel size as the corresponding SPECT images. Consecutive pairs of positron emission tomographic slices were combined to achieve an identical axial pixel size for positron emission tomography and SPECT imaging.

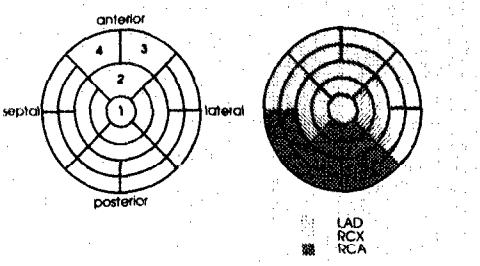

Figure 1. The "polar target" of the left ventricle from apex (center region, 1) to base (outer circle region, 4). The **upper part** represents the anterior wall, the **lower part** the posterior wall, with the septal **left** and the lateral wall of the left ventricle at the **right side**. Regional uptake of technetium-99m sestamibi by SPECT and fluorine-18 fluorodeoxyglucose by positron emission tomography was expressed as percent to the region of maximal perfusion (100%). For this study, only data in the left anterior descending coronary (LAD) territory were assessed with exclusion of the septal region. RCA = right coronary artery; RCX = circumflex artery.

Analysis of SPECT imaging and positron emission tomographic data. The transaxial positron emission tomographic image files were converted to the structure of the SPECT imaging files and transferred to the MaxDelta system using a local area network. Regional Tc-99m sestamibi and F-18 fluorodeoxyglucose uptake were expressed in percent of the uptake in the region with maximal sestamibi uptake (27) (Fig. 1). A concordant sestamibi reduction <50% and fluorodeoxyglucose uptake <50% was defined as a scar, whereas reduced sestamibi uptake but preserved fluorodeoxyglucose activity (>70%) represented a perfusion/metabolism mismatch (28).

Coronary revascularization. Coronary artery bypass surgery was performed by use of standard techniques under cardioplegic condition with internal mammary artery grafting to the left anterior descending coronary artery. Surgeons attempted to perform complete revascularization if technically feasible. The interval between coronary angiography and surgical revascularization was 4 ± 2 weeks.

Myocardial biopsy sampling. Transmural needle biopsy specimens were obtained during coronary artery bypass sur-

Table 1. Morphologic Group Characteristics

	Group 1 (n = 11)	Group 2 (n = 13)
Contractile material	Number reduced	Number and normal pattern severely altered
Titin and alpha-actinin	Slightly reduced	Significantly reduced
t-tubular system	Normal	Dilated
Shape of nuclei	Normal	Invaginations, inclusions
Size of nuclei	Normal	Enlarged
Mitochondria	Majority normal	Altered size, cristae reduction
Glycogen	Modest amounts	Large amounts
Vacuoles; myelin figures, lipofuscin, fat droplets	Occasional findings	Overall increased
Fibrotic tissue	Modestly enhanced (<30%)	Severely augmented (>30%)

Group 1 = patients with only minor degenerative changes; Group 2 = patients with severe degenerative deterioration of the cell architecture.

gery using a Tru-Cut needle 2N 27004T (Travenol Laboratories, Inc.). The region of interest for the intraoperative biopsy sampling was preoperatively defined from left ventricular angiograms. Two biopsy specimens per patient were taken with a total wet weight of 10 to 40 mg after the heart was suspended in a pericardial cradle and just before induction of cardiac arrest by cardioplegic solution. Biopsy specimens were taken only from the center of the wall motion abnormality.

Tissue preparation for electron microscopy. Each biopsy specimen was divided into a subendocardial and a subepicardial part and was fixed in cold 3% glutaraldehyde in cacodylatebuffer (pH 7.4, 400 mOsm). After immersion fixation, the biopsy specimens were washed in cacodylatebuffer 0.1 M plus sodium cacodylate, 7.5% saccharose, pH 7.4. The samples were embedded in Epon after fixation in 2% osmic acid tetroxide and were dehydrated in ethanol plus substitution by propylene oxide using an automatic tissue processor. Thin sections (50 to 60 nm) were studied by electron microscopy.

Tissue preparation for immunohistochemical analysis. For immunohistochemical analysis, the second tissue biopsy specimen was immediately frozen in liquid nitrogen and stored at −80°C. Cryostate sections of 4-μm thickness were prepared, fixed in acetone and incubated in the first antibody—either titin T12, alpha-actinin (Sigma) or collagen VI (Telios/Klon A 112)—for 45 min. The second antibody, biotinylated goat antimouse or donkey antirabbit (Amersham), was then applied for 45 min; and finally, fluoresceinisothiocyanat-labeled streptavidin (Amersham) was added. The sections were mounted in Mowiol (Hoechst) and studied using a Leica Aristoplan microscope equipped for fluorescence microscopy.

Morphometric analysis. The degree of fibrosis was determined by morphometric techniques using the point counting method (29). Values are indicated as percentage of the whole biopsy tissue.

Definition of the patient groups. Patients were retrospectively divided into two groups (Table 1) depending on the results of the morphologic analysis and on the degree of structural degeneration. Group 1 (n = 11) represented patients with only minor ultrastructural changes, a normal or near-normal shape and size of intracellular organelles, only slightly reduced amounts of contractile material and a modest occurrence of fibrotic tissue. In group 2 (n = 13), patients showed severe ultrastructural signs of degeneration, increased amounts of abnormal intracellular particles, significantly reduced and altered myofilaments and an increased degree of fibrosis (>30%).

Statistical analysis. All values are expressed as mean ± SD. Statistical comparisons were made using the paired Student *t* test. A p value <0.05 was considered statistically significant.

Results

Patient data and clinical follow-up. All patients had multivessel disease (21 triple-vessel, 3 double-vessel coronary artery disease) with a significant left anterior descending coronary artery stenosis (>70%) or occlusion. No differences were found between the two groups concerning demographic and clinical data. Preoperatively, all patients had severe angina and belonged to class III or IV of the Canadian Cardiovascular Society (CCS) classification. At 6-month follow-up, angina in all patients lessened at least by one CCS grade. Symptoms of heart failure also lessened substantially at follow-up. According to the New York Heart Association classification, 10 patients had only mild preoperative symptoms (class II), whereas 14 patients were in class III or IV. After coronary artery bypass surgery, all patients were either asymptomatic or in class I or II. Functional outcome did not differ between the two groups.

Morphology. The location of a small metal clip, intraoperatively sutured at the side of tissue sampling, was compared with its location at follow-up angiography with the regional wall motion abnormality at baseline angiography and demonstrated good agreement between the biopsy location and angiographically defined dysfunction.

Electron microscopy. Viable myocytes were found in all biopsy samples from the dyscontractile regions. There was no evidence for previous transmural infarction. The cardiac myocytes, however, showed signs of severe degeneration with loss of myofilaments, occurrence of cellular sequestration, decreased sizes of mitochondria and cellular debris. An increased degree of extracellular fibrosis was present (Fig. 2 and 3). The myocyte nuclei were abnormally shaped and sized and displayed cytoplasmatic inclusions or the occurrence of fine filaments. The mitochondria had a different appearance; many were small; and some showed a reduced number of cristae. Other abnormalities, such as presence of glycogen deposits, fat droplets, lipofuscin and degenerative vacuoles, were common.

Immunohistochemical analysis. Titin and alpha-actinin staining was used to study alterations of the contractile appa-

Figure 2. A, Lack of contractile material in a peripheral part of a myocyte filled with glycogen (GL). The extracellular space is widened and contains macrophages (M) and cellular debris (CD). An endothelial cell is present in the upper part (End). ×2,900, reduced by 35%. B, Alterations of a cardiomyocyte in hibernating myocardium. The contractile material (CM) is diminished and replaced by nonspecific cytoplasm (NC), and the nucleus (N) exhibits a multilobular shape. ×4,300, reduced by 35%.

Figure 3. A, Sequestration of cellular particles (CP) from myocytes into the extracellular space, leading to final atrophy of the cells. ×21,500, reduced by 35%. B, Atrophied cardiomyocyte containing minimal amounts of contractile material (CM), abnormal mitochondria and multiple vacuoles. The cellular debris is surrounded by fibrotic material. ×6,450, reduced by 35%.

ratus of the cardiomyocytes. These proteins closely connect with myosin and actin, respectively, and represent changes of the myofilaments. The most obvious finding was the loss of structures representing these contractile proteins, which confirms the ultrastructural findings of myofilament reduction. These defects were of different degrees of severity, and the changes were graded as either slight or severe (Fig. 4 and 5). The occurrence of small parts of atrophied cells or of cellular debris could also be demonstrated by staining for these intracellular proteins. Staining for collagen VI was used as an indicator of the degree of fibrosis. The degree of fibrosis also was graded as slight versus severe alterations (Fig. 6).

Morphometry. The amount of fibrosis, as assessed by morphometric quantitative analysis, was 21 ± 9% in group 1 compared with 45 ± 15% in group 2 ($p < 0.05$). In both groups, the occurrence of fibrosis was significantly higher in the subendocardial than in the subepicardial specimen (36 ± 17% vs. 22 ± 11%, $p < 0.05$).

Loss of contractile material and the severity of fibrosis assessed by immunohistochemical staining paralleled the de-

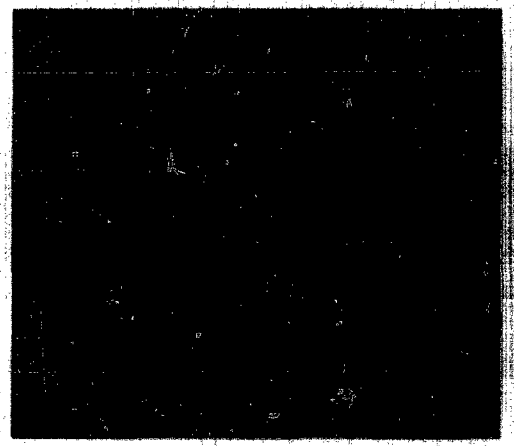

Figure 4. Immunostaining for titin in hibernating myocardium. Specific fluorescence is green, the nuclei are red, and lipofuscin is yellow. The myocytes are of different shapes and sizes and show a reduction of the contractile material (right-hand side) and an occurrence of small cellular particles in the enlarged extracellular space. ×530, reduced by 30%.

gree of degenerative changes detected by electron microscopy in each patient. Those patients with most severe ultrastructural alterations displayed most degenerative changes when immunohistochemical staining was used, indicating a good correlation between both methods.

Angiographic results. Seventeen of 24 patients (71%) had significant left anterior descending coronary artery stenosis (>70% diameter reduction). The remaining seven patients (29%) had total occlusion of the left anterior descending coronary artery with angiographically visible collateral channels. Baseline ejection fraction was 44 ± 12% (range 26% to 59%). All patients had hypokinesia or akinesia of the anterior wall including the septum and apex (Table 2). The severity of coronary stenosis did not correlate with the ultrastructural findings. In particular, those patients with occluded vessels did not demonstrate more severe degenerative changes or more disruption of the cytoskeleton. Also, the severity of wall motion abnormalities neither correlated with the angiographic degree of stenosis nor with structural changes.

Twenty of 24 patients (83%) had follow-up angiography 6 ± 1 months after coronary artery bypass surgery. Postoperative ejection fraction (Table 2) improved in all patients from 44 ± 12% to 54 ± 9% ($p < 0.05$). Wall motion abnormality in the left anterior descending coronary artery center improved from −2.1 ± 0.7 to −1.3 ± 0.6 ($p < 0.05$) (Fig. 7). However, the degree of functional recovery at follow-up did not correlate with the ultrastructural findings.

Nuclear perfusion and metabolism imaging. Nuclear imaging did not reveal significant differences between the two groups defined by morphologic alterations. All patients had perfusion defects in the anterior wall (group 1: 54 ± 6%; group 2: 56 ± 6%) without a significant difference for those with a

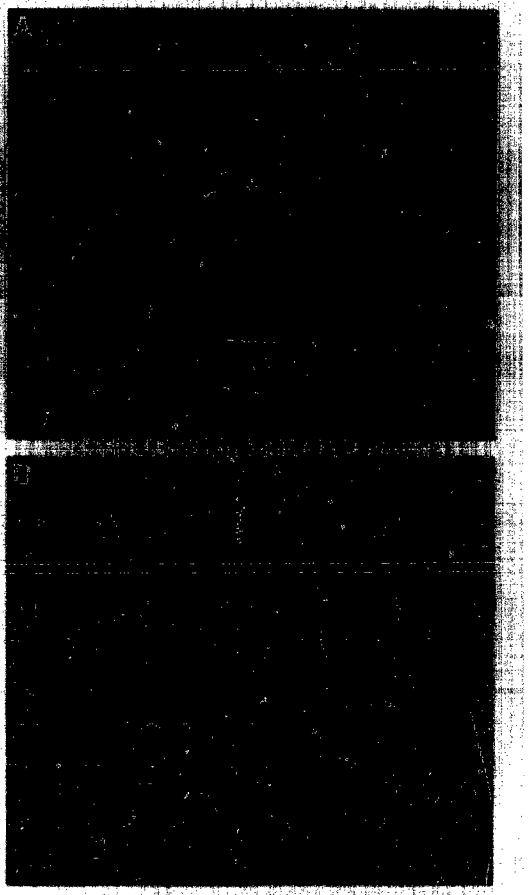

Figure 5. A, Immunostaining for alpha-actinin in normal human myocardium. Note the regular cross striation. ×530, reduced by 30%. B, Staining for alpha-actinin in hibernating myocardium shows the lack of contractile material and the irregular arrangement of the remaining sarcomeres. Several cells are hypertrophied (upper left corner); others are slender and atrophied (lower part). ×530, reduced by 30%.

stenosed left anterior descending coronary artery (n = 17, sestamibi uptake 55 ± 5%) and for those with left anterior descending coronary artery occlusion (n = 7, sestamibi uptake = 50 ± 7). Quantitative assessment of the normalized positron emission tomographic data showed a mismatch between perfusion and metabolism in all patients in the anterior wall. Average F-18 deoxyglucose uptake in the anterior wall measured 87 ± 11% in group 1 and 88 ± 9% in group 2, indicating persistent viability (Fig. 8).

Discussion

The presented results indicate that myocardial hibernation—defined from postrevascularization functional recovery of previously dyscontractile myocardium and from preopera-

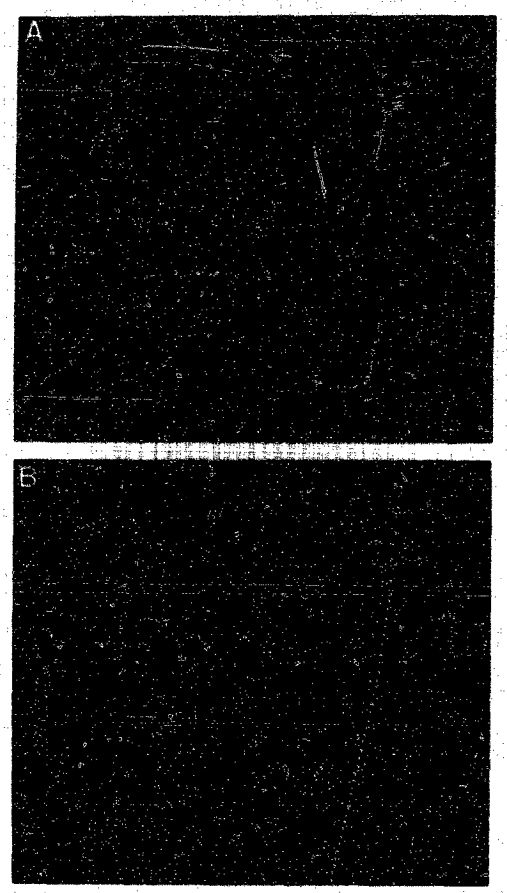

Figure 6. Immunostaining for collagen VI. A, The extracellular space between myocytes is filled with small amounts of collagen, characteristic for group 1. ×210, reduced by 30%. **B,** A significantly increased amount of collagen VI is located between myocytes, separating them from each other. This is a severe alteration. **Dark areas** represent myocytes in both **A** and **B**. ×210, reduced by 30%.

tive viability imaging—do not represent a uniform morphologic appearance.

Various degrees of degenerative changes and loss of contractile material were associated with similar preoperative perfusion and metabolic alterations and functional outcome after restoration of blood flow. Even in patients with severe structural abnormalities, functional recovery can be achieved if the myocardium is still hibernating. On the other hand, functional abnormalities do not distinguish between moderate and severe degenerative alterations of the myocardium as proved by histologic and immunohistochemical analyses.

In the present study, all patients with successful revascularization of the left anterior descending coronary artery showed preoperative wall motion abnormalities, reduced coronary blood flow but persistent glucose uptake and functional recovery after revascularization. One group of patients demonstrated only slight or moderate degenerative alterations and slightly reduced contractile proteins, normal cellular organelles and the presence of only a moderate degree of fibrosis. In the second group of patients, severe structural alterations were present including degenerative changes of the myocytes, atrophy, occurrence of sequestered cellular particles, severe disorganization of the cytoskeleton with decreased contractile proteins in the extracellular space and the presence of more severe fibrosis.

Compared with previously published studies on morphologic changes in myocardial hibernation (18,22,23), the present analytical approach classifies, for the first time, patients into two groups depending on the morphologic findings. These findings displayed a varied appearance of structural degeneration in a particular myocardial area with regional hypokinesia. Because the differences in structural appearance of the biopsy specimens were obvious, that is, normal morphologic appearance or slight versus severe alterations, the division into two groups seemed reasonable.

The most important finding was that all biopsy specimens showed signs of long-term degeneration, most probably due to ischemia, without evidence of transmural infarction. Interestingly, the severity of the morphologic changes did not correlate with regional wall motion abnormalities, with different fluorodeoxyglucose uptake, nor with the functional or clinical outcome.

Pathophysiologic implications. Severe wall motion abnormalities of long-term hypoperfused myocardium can be present in the absence of severe tissue injury. In these cases, the adaptation process, as defined in the earlier descriptions, is comparable with the situation of short hibernation known from animal experiments (30,31). Active downregulation of the contractile function due to a downregulation of myocardial oxygen consumption (32) may occur in these patients and probably represents the early stage of hibernation. This process may involve repetitive stunning, but this is almost impossible to clarify in the human heart. Myofilaments are still present, but they are not active in contraction. This process might involve altered Ca^{2+} fluxes or potassium pump activity (33). It is also possible that in functionally downregulated myocytes, mRNA synthesis rate for contractile proteins is much lower than that in normally contracting myocytes, as was shown in vascular smooth muscle cells (34), which may lead to changes in contractile protein enzyme activity (35).

The more severe structural alterations in the second group may represent a more advanced stage of the disease, that is, a partial exhaustion of the cellular adaptation causing hibernation and the occurrence of degeneration and final cell death. In contrast, a recent study by Flameng and Shivalkar (36) described end-stage hibernation in patients without functional recovery after revascularization. However, structural and functional end stage of chronic ischemia and the exact time-point of no return of function due to the loss of downregulation capacities may overlap and cannot be distinguished by indirect imaging techniques.

Table 2. Left Ventricular Ejection Fraction and Regional Wall Motion Abnormalities (before and after revascularization)*

	Group 1		Group 2		All Patients	
	Before	After	Before	After	Before	After
Ejection fraction (%)	46.6 ± 11.3	56.6 ± 8.5†	43.5 ± 13.3	53.0 ± 10.0†	44 ± 12	54.3 ± 9†
WMA LAD						
Center SD	−2.0 ± 0.7	−1.4 ± 0.8†	−2.1 ± 0.6	−1.2 ± 0.5†	−2.1 ± 0.7	−1.3 ± 0.6†
Periphery SD	−1.5 ± 0.3	−0.8 ± 0.5	−1.4 ± 0.4	−1.1 ± 0.5	−1.4 ± 0.5	−1.0 ± 0.7

*Determined by the centerline method and expressed in units of standard deviation of the normal mean (mean ± 1 SD) of the left anterior descending coronary artery (LAD) region. Center represents the worst 50% of chords of the anterior wall, whereas periphery represents the remaining chords. There were no significant differences in the baseline data between the two groups. Postoperatively, ejection fraction and the center of regional wall motion abnormality (WMA) improved in both groups (†$p < 0.05$ vs. preoperative data).

Evaluation of ultrastructural and immunohistochemical techniques. Electron microscopy permits the evaluation of the subcellular organelles but it does not allow detection of cytoskeletal elements associated with the contractile apparatus such as titin and alpha-actinin. Titin and alpha-actinin are of special interest because these proteins are important for the sarcomere structure (37) and for sarcomerogenesis (38,39). A lack of titin, therefore, is most probably the basis of disturbed sarcomerogenesis and of the absence of contractile material. The immunohistochemical techniques allow to characterize the conditions of the contractile apparatus of the cardiomyocytes, which are variably altered in long-term hibernating myocardium and represent more a substantial degeneration of the cytoskeleton. The two morphologic methods used in our study, electron microscopy and immunohistochemical analysis, showed an impressive similarity in the structural appearance and the severity of changes in the hibernating myocardium.

Clinical implications. The degree of degenerative injury is more than expected from previous studies demonstrating immediate functional recovery after revascularization (15). However, recent data on the time course of function after revascularization suggest a delayed recovery of contractile function (4,40). If so, hibernating myocardium may represent an adaptive process insufficient to maintain cell integrity for the entire hypoperfused myocardium. Not all myocardial cells can survive, and functional recovery is partially incomplete or delayed, or both.

That patients with slight morphologic changes also showed only partial recovery of regional function supports the existence of different states of long-term adaptation in the same heart. Long-term observations may result in further recovery as it has been described by serial evaluation after either coronary angioplasty (4) or coronary artery bypass surgery

Figure 7. Central regional wall motion (WMA center) at baseline (pre) and after coronary revascularization (post) for both groups (**A** and **B**).

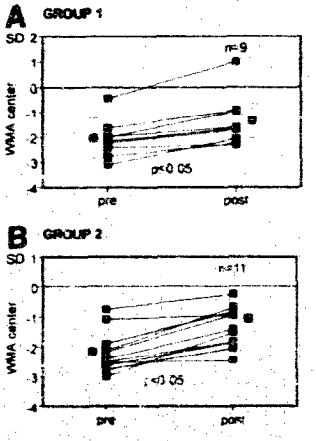

Figure 8. a, Technetium-99m (Tc 99m) sestamibi uptake for both groups from apex (area 1) to base (area 4). Compared with the individual maximal perfusion of 100%, all patients showed reduced perfusion in the anterior wall. No significant differences were found between the patients with only minor (group 1) and those with severe ultrastructural changes (group 2). **b,** Fluorine-18 fluorodeoxyglucose (FDG) uptake for both groups from apex to base (area 4) of the anterior wall. There were no significant differences between the two groups. PET = positron emission tomography; SPECT = single-photon emission computed tomography.

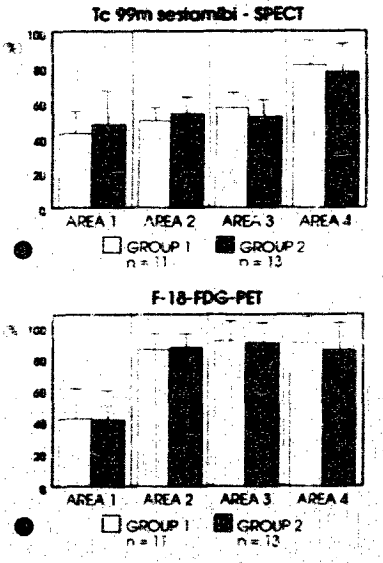

(40). However, evaluation of the time-course of this degeneration was not part of this study design and may vary substantially among patients.

The findings from transmural biopsy specimens did not demonstrate any predictive power for a therapeutic strategy. Furthermore, nuclear imaging techniques cannot distinguish between mild and severe structural damages in dyscontractile but viable tissue.

Study limitations. Our data were obtained from a relatively small number of patients with evidence for hibernating myocardium. Owing to logistic reasons, we were not able to provide data on absolute myocardial blood flow without an on-site cyclotron. However, from the clinical point of view, perfusion imaging using Tc-99m sestamibi in combination with semiquantitative SPECT imaging analysis is a widely accepted method (41).

Conclusions. The protective mechanisms of hibernating myocardium seem to be insufficient in the presence of persistent underperfusion or with the occurrence of multiple ischemic episodes. Cardiac structure deteriorates, finally leading to cell death and fibrosis. This seems to be a progressive and probably time-dependent process or may even reflect different conditions of the myocytes. Thus, early coronary revascularization might be the only therapeutic strategy that could avoid structural degeneration or that could even result in functional and morphologic restitution.

We gratefully acknowledge the helpful comments of Bharati Shivalkar, MD, University of Leuven, Belgium.

References

1. Rahimtoola SH. A perspective on the three large multicenter randomized clinical trials of coronary bypass surgery for chronic stable angina. Circulation 1987;75 Suppl V:V123–35.
2. Rahimtoola SH. The hibernating myocardium. Am Heart J 1989;117:211–21.
3. Ross J Jr. Myocardial perfusion-contraction matching. Circulation 1991;83: 1076–83.
4. Nienaber CA, Brunken RC, Sherman CT, et al. Metabolic and functional recovery of ischemic human myocardium after coronary angioplasty. J Am Coll Cardiol 1991;18:966–78.
5. Cohen M, Charney R, Hershman R, Fuster V, Gorlin R, Francis X. Reversal of chronic ischemic myocardial dysfunction after transluminal coronary angioplasty. J Am Coll Cardiol 1988;12:1193–8.
6. van den Berg EKJ, Popma JJ, Dehmer DJ, et al. Reversible segmental left ventricular dysfunction after coronary angioplasty. Circulation 1990;81: 1210–6.
7. vom Dahl J, Uebis R, Sheehan FH, et al. Factors influencing outcome of regional wall motion after successful elective single-vessel percutaneous transluminal coronary angioplasty. Cor Art Dis 1992;3:489–98.
8. Rees G, Bristow JD, Kremkau EL, et al. Influence of aortocoronary bypass surgery on left ventricular performance. N Engl J Med 1971;284:1116–20.
9. vom Dahl J, Eitzman DT, Al-Aouar R, et al. Relationship of regional function, flow and metabolism in patients with advanced coronary artery disease undergoing surgical revascularization. Circulation 1994;90:2356–66.
10. Chatterjee K, Swan HJC, Parmley WW, Sustaita H, Marcus HS, Matloff J. Influence of direct myocardial revascularization on left ventricular asynergy and function in patients with coronary heart disease. Circulation 1973;47: 276–86.
11. Shivalkar B, Borgers M, Maes A, Mortelmans L, Flameng W. Low regional function associated with high metabolism predicts functional recovery after coronary bypass surgery [abstract]. Circulation 1994;90 Suppl I:I-251.
12. Tillisch J, Brunken R, Marshall R, et al. Reversibility of cardiac wall motion abnormalities predicted by positron tomography. N Engl J Med 1986;314: 884–8.
13. Tamaki N, Yonekura Y, Yamashita K, et al. Positron emission tomography using fluorine-18 deoxyglucose in evaluation of coronary artery bypass grafting. Am J Cardiol 1989;64:860–5.
14. Knuuti MJ, Saraste M, Nuutila P, et al. Myocardial viability: fluorine-18-deoxyglucose positron emission tomography in prediction of wall motion recovery after revascularization. Am Heart J 1994;127:785–96.
15. Topol EJ, Weiss JL, Guzman PA, et al. Immediate improvement of dysfunctional myocardial segments after coronary revascularization: detection by intraoperative transesophageal echocardiography. J Am Coll Cardiol 1984;4:1123–34.
16. Marwick TH, MacIntyre WJ, Lafont A, Nemec JJ, Salcedo EE. Metabolic responses of hibernating and infarcted myocardium to revascularization. A follow-up study of regional perfusion, function, and metabolism. Circulation 1992;85:1347–53.
17. Thiedemann KU. Ultrastructure in chronic ischemia, studies in human hearts. In: Schaper W, editor. The Pathophysiology of Myocardial Perfusion. Amsterdam: Elsevier/North-Holland Biomedical Press, 1979:675–716.
18. Borgers M, Thone F, Wouters L, Ausma J, Shivalkar B, Flameng W. Structural correlates of regional myocardial dysfunction in patients with critical coronary artery stenosis: chronic hibernation? Cardiovasc Pathol 1993;2:237–45.
19. Flameng W, Suy R, Schwartz F, et al. Ultrastructural correlates of left ventricular contraction abnormalities in patients with chronic ischemic heart disease: determinants of reversible segmental asynergy post revascularization surgery. Am Heart J 1981;102:846–57.
20. Flameng W, Wolters L, Sergeant P, et al. Multivariate analysis of angiographic, histologic, and electrocardiographic data in patients with coronary heart disease. Circulation 1984;70:7–17.
21. Shivalkar B, Borgers M, Daenen W, Gewillig M, Flameng W. ALCAPA syndrome: an example of chronic myocardial hypoperfusion? J Am Coll Cardiol 1994;23:772–8.
22. Vanoverschelde JLJ, Wijns W, Depre C, et al. Mechanisms of chronic regional postischemic dysfunction in humans. New insights from the study of noninfarcted collateral-dependent myocardium. Circulation 1993;87:1513–23.
23. Maes A, Flameng W, Nuyts J, et al. Histological alterations in chronically hypoperfused myocardium. Correlation with PET findings. Circulation 1994; 90:735–45.
24. Dodge HT, Sandler H, Baxley WA, Hawley RR. Usefulness and limitations of radiographic methods for determining left ventricular volumes. Am J Cardiol 1966;18:10–24.
25. Sheehan FH, Bolson EL, Dodge HT, Mathey DG, Schofer J, Woo HW. Advantages and applications of the centerline method for characterizing regional ventricular function. Circulation 1986;74:293–305.
26. Jeppson GM, Clayton PD, Blair TJ, Liddle HV, Jensen RL, Klausner SC. Changes in left ventricular wall motion after coronary bypass surgery: signal or noise? Circulation 1981;64:945–51.
27. Altehoefer C, Kaiser HJ, Doerr R, et al. Fluorine-18 deoxyglucose PET for assessment of viable myocardium in perfusion defects in 99mTc-MIBI SPECT: a comparative study in patients with coronary artery disease. Eur J Nucl Med 1992;19:334–42.
28. Altehoefer C, vom Dahl J, Biedermann M, et al. Relationship between defect severity of Tc-99m isonitrile SPECT and FDG PET for assessment of myocardial viability in patients with coronary artery disease. J Nucl Med 1994;35:569–74.
29. Weibel ER, Elias H. Introduction to stereologic principles. In: Weibel ER and Elias H, editors. Quantitative Methods in Morphology. New York: Springer Verlag, 1967.
30. Schulz R, Guth BD, Pieper K, Martin C, Heusch G. Recruitment of an inotropic reserve in moderately ischemic myocardium at the expense of metabolic recovery: a model of short-term hibernation. Circ Res 1992;70: 1282–95.
31. Schulz R, Rose J, Martin C, Brodde OE, Heusch G. Development of short term myocardial hibernation: its limitation by the severity of ischemia and inotropic stimulation. Circulation 1993;88:684–95.
32. Canty JM, Fallavollita JA. Hibernating myocardium represents a primary downregulation of regional myocardial oxygen consumption distal to a critical coronary stenosis. Basic Res Cardiol 1995;90:5–8.

33. Steenbergen C, Fralix TA, Murphy E. Role of increased cytosolic free calcium concentration in myocardial ischemic injury. Basic Res Cardiol 1993;88:456–70.
34. Nomura K, Teraoka H, Arita H, Ohara O. Disorganization of microfilaments is accompanied by downregulation of alpha-smooth muscle actin isoform mRNA level in cultured vascular smooth muscle cells. J Biochem (Tokyo) 1992;112:102–6.
35. Capasso JM, Malhotra A, Li P, Zhang X, Scheuer J, Anversa P. Chronic nonocclusive coronary artery constriction impairs ventricular function, myocardial structure, and cardiac contractile protein enzyme activity in rats. Circ Res 1992;70:148–62.
36. Flameng W, Shivalkar B. Hibernating myocardium, a clinical entity. Basic Res Cardiol 1995;90:55–7.
37. Hein S, Scholz D, Fujitani N, et al. Altered expression of titin and contractile proteins in failing human myocardium. J Mol Cell Cardiol 1994;26:1291–306.
38. Isaacs WB, Kim IS, Struve A, Fulton AB. Biosynthesis of titin in cultured skeletal muscle cells. J Cell Biol 1989;109:2189–95.
39. Isaacs WB, Kim IS, Struve A, Fulton AB. Association of titin and myosin heavy chain in developing skeletal muscle. Proc Natl Acad Sci USA 1992;89:7496–500.
40. Vanoverschelde JL, Melin JA, Depre C, Borgers M, Dion R, Wijns W. Time course of functional recovery of hibernating myocardium after coronary revascularization [abstract]. Circulation 1994;90 Suppl I:I-378.
41. Maddahi J, Kiat H, Berman DS. Myocardial perfusion imaging with technetium-99m-labeled agents. Am J Cardiol 1991;67:27–34D.